Corrosion Resistance of Murataite-Based Ceramics Containing Simulated Actinide/Rare Earth Fraction of High Level Waste - 9299

S.V. Stefanovsky, G.A. Varlakova, O.A. Burlaka, O.I. Stefanovsky
State Unitary Enterprise SIA Radon
7th Rostovskii lane 2/14, Moscow 119121 RUSSIA

B.S. Nikonov, S.V. Yudintsev
Institute of Geology of Ore Deposits, Petrography, Mineralogy and Geochemistry of the Russian Academy of Sciences (IGEM RAS)
Staromonetny lane 35, Moscow 119117 RUSSIA

ABSTRACT

Two samples of murataite-based ceramics containing simulated Actinide/Rare Earth (An/RE) fraction of high level waste (HLW) produced by a cold crucible inductive melting (CCIM) were tested using a single-pass-flow-through (SPFT) procedure. As-prepared and leached samples were examined by X-ray diffraction (XRD) and scanning electron microscopy with energy dispersive system (SEM/EDS). The as-prepared ceramics were composed of murataite, perovskite and crichtonite as well as minor zirconolite and rutile (in one sample). Elemental concentrations at pH=2 and T=90°C were measured and leach rates were calculated. Perovskite concentrating Ca and Ce-group REs (La, Ce, Pr, Nd) was found to be the lowest durable phase. Leach rates of Ca and Ce-group REs (Ce, Nd) from the sample with higher perovskite content were found to be higher than those of U and Zr by one to three orders of magnitude. Elemental leach rates from the ceramic with lower perovskite content are lower by up to 10 times.

INTRODUCTION

Among the candidate actinide host phases, murataite, more exactly polytypes of the murataite/pyrochlore series, whose structures are built from nano-sized pyrochlore (two-fold fluorite unit cell) and murataite (three-fold fluorite unit cell) blocks (modules), is considered to be one of the most perspective for immobilization of complex actinide-bearing wastes [1]. Unlike the pyrochlore structure having two cationic sites: eight-coordinated A^{VIII} and six-coordinated B^{VI}, the murataite structure has four distinct cationic sites: eight-coordinated A^{VIII}, octahedrally-coordinated B^{VI}, five-coordinated (trigonal bipyramid) C^{V}, and four-coordinated (tetrahedron) T^{IV} [2] allowing to accommodating of waste elements with wide variety of cationic radii and charges. Large-sized actinides (Th, U, Np, Pu, Am, Cm), rare earths (RE = Y, La…Gd, Zr, Hf, Nb), Na, Ca occupy the A^{VIII} sites, whereas smaller-sized Ti, Fe and Fe-group elements, Al, Ga enter the B^{VI} sites. The C^{V} sites are filled with Mn, Fe, Ti, and Zn (the latter in the naturally-occurred samples only). Mn is partitioned between the A^{VIII} and C^{V} sites, at that, Mn^{2+} ions enter predominantly the A^{VIII} and $Mn^{3+/4+}$ ions occupy the C^{V} sites. The T^{IV} sites are filled with small-sized cations (Zn^{2+}, Si^{4+}) in the naturally-occurred samples and normally empty in the synthetic phases. Currently the murataite formula is written as $A^{VIII}{}_3B^{VI}{}_6C^{V}{}_2O_{20-x}$ or $A^{VIII}{}_3B^{VI}{}_6C^{V}{}_2O_{22-x/2}$. Combining the formulae of murataite and pyrochlore ($A^{VIII}{}_2B^{VI}{}_2O_{7-x}$) the formulae of the polytypes with five- ($A^{VIII}{}_5B^{VI}{}_8C^{V}{}_2O_{27-x}$), seven- ($A^{VIII}{}_7B^{VI}{}_{10}C^{V}{}_2O_{34-x}$) and eight-fold elementary fluorite unit cells ($A^{VIII}{}_8B^{VI}{}_{14}C^{V}{}_4O_{47-x}$) have been derived [1,3]. Murataite-containing polytypes form grains with a zoned structure. Core and rim of the grains are normally composed of the polytypes with five- (5C or M5) and eight-fold (8C or M8) cubic fluorite unit cell, respectively. These grains are surrounded by the "normal" murataite with three-fold fluorite cell (3C or M3). Content of actinide and rare earth elements is the highest in the core and reduces towards "normal" murataite. Zoned distribution of these elements in the murataite grains prevents their release into leachate and the environment [1].

The major problem is production of "single phase" murataite ceramics. Maximum content in the murataite-based ceramics ever reached was found to be ~95 wt%. Extra phases were perovskite, crichtonite, pyrophanite/ilmenite, and rutile. The most troublesome phase is perovskite concentrating light (Ce-group) REs (La…Nd) and capable to incorporate isomorphically traces of trivalent actinides (Pu, Am, Cm) and whose chemical durability is much lower than the "murataite". In our previous work [4] we produced a ceramic containing an An/RE fraction surrogate with baseline "murataite" composition (wt%): 5 Al_2O_3, 10 CaO, 55 TiO_2, 10 MnO, 5 Fe_2O_3, 5 ZrO_2, 10 An/REE fraction, and found that the content of each of the "murataite" and perovskite phases was 35-40 % of total, secondary in abundance crichtonite – 15-20 % of total, and minor pyrophanite/ilmenite – ≤ 5 % of total. In order to shift the phase assemblage in favor of "murataite" we added extra TiO_2 and ZrO_2 (3:1 ratio, 25 wt% of total). This reduces perovskite formation and increases "murataite" content. At that, zirconolite was one more extra phase found in the ceramic. However, this phase has excellent chemical and radiation resistance and its occurrence in the ceramics does not create problems.

In the present work we studied corrosion resistance of these two murataite-based ceramics (Table 1) produced by CCIM with various phase composition using a single-pass-flow-through (SPFT) procedure [5].

EXPERIMENTAL

Process variables at CCIM production, XRD and SEM/EDS examination of the as-prepared ceramics labeled as 2c and 4c were described in details in our previous paper [4]. The specimens for SPFT testing were sampled from the core of the ingots. The measured densities of the ceramics 2c and 4c were 3.40 g/cm^3 and 3.55 g/cm^3, respectively.

The SPFT test was performed in an apparatus (Figure 1) delivered by Pacific Northwest National Laboratory, USA, under a contract between US DOE and SIA Radon. The procedure based on contact between powdered specimen and continuously flowing leachant at various temperatures and pH values is close to a MCC-4 test and described in details in several works (see, for example, [5,6]).

Major parameters of our tests were as follows: temperature - 90±2 °C, leachant – 0.01 M HNO_3 solution, leachant flow rate – 3 mL/hr (8.33 10^{-10} m^3/s). The particle size ranged between 75 and 150 μm. Solutions were analyzed by ICP-AES using a Perkin-Elmer Optima 4300 DV spectrometer. Leach rates of Ca, Zr, Ce, Nd, and U were calculated as described in refs. [5,6]:

$$r_i = [(C_i - C_0)\, q]/(f\, S)$$

where r_i = the normalized leach rate (g/m^2 d) of the element i, C_i = the concentration (g/m^2) of the element *i* in the effluent, C_0 = the average background concentration (g/m^2) of the element i, q = the flow rate (m^3/d) of the effluent, f = the mass fraction of the element *i* in the ceramic, S = the average specific surface area (m^2) of the specimen.

Table I. Brief characterization of the murataite-based ceramics produced by CCIM.

Target oxide content, wt%	Oxides	Sample 2c	Sample 4c
	Al_2O_3	5.0	4.0
	CaO	10.0	8.0
	TiO_2	55.0	59.0
	MnO	10.0	8.0
	Fe_2O_3	5.0	4.0
	ZrO_2	4.0	8.2

	La_2O_3	1.25	1.0
	Ce_2O_3	2.48	1.98
	Pr_6O_{11}	1.23	0.98
	Nd_2O_3	3.96	3.17
	Sm_2O_3	0.73	0.59
	Eu_2O_3	0.20	0.16
	Gd_2O_3	0.15	0.12
	UO_2	1.0	0.8
Actual phase content, vol%	"Murataite"	35-40	55-60
	Perovskite	35-40	10-15
	Crichtonite	20-25	15-20
	Pyrophanite/Ilmenite	≤5	-
	Zirconolite	-	≤5
	Rutile	-	10-15
Density, g/cm^3		3.40	3.55

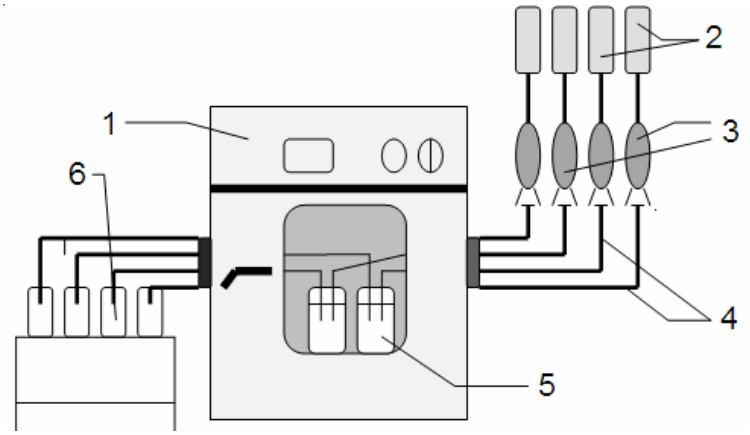

Figure 1. Schematic representation of the SPFT apparatus used to test the corrosion durability of the murataite-based ceramics.

1 – oven, 2 – vessels for leaching solutions, 3 – pumps, 4 – solution feeding lines, 5 – reactor vessels, 6 – collection bottles.

RESULTS

Leaching parameters, elemental concentrations and normalized elemental leach rates are shown in Tables 2 and 3. For the sample 2c average normalized elemental leach rates were found to be ($g\ m^{-2}\ d^{-1}$): $1.50 \cdot 10^{-1}$ for Ca, $1.19 \cdot 10^{-1}$ for Ce, $1.33 \cdot 10^{-1}$ for Nd, $1.55 \cdot 10^{-2}$ for U, and $4.85 \cdot 10^{-5}$ for Zr. For the sample 4c with modified chemical and phase compositions they were ($g\ m^{-2}\ d^{-1}$) $3.93 \cdot 10^{-2}$ for Ca, $2.21 \cdot 10^{-2}$ for Ce, $2.39 \cdot 10^{-2}$ for Nd, $3.39 \cdot 10^{-3}$ for U, and $2.73 \cdot 10^{-5}$ for Zr. Plots of $\log_{10} r_i$ versus test duration (Figure 2) demonstrate rather fast achieving of equilibrium state for all the elements leached except Zr.

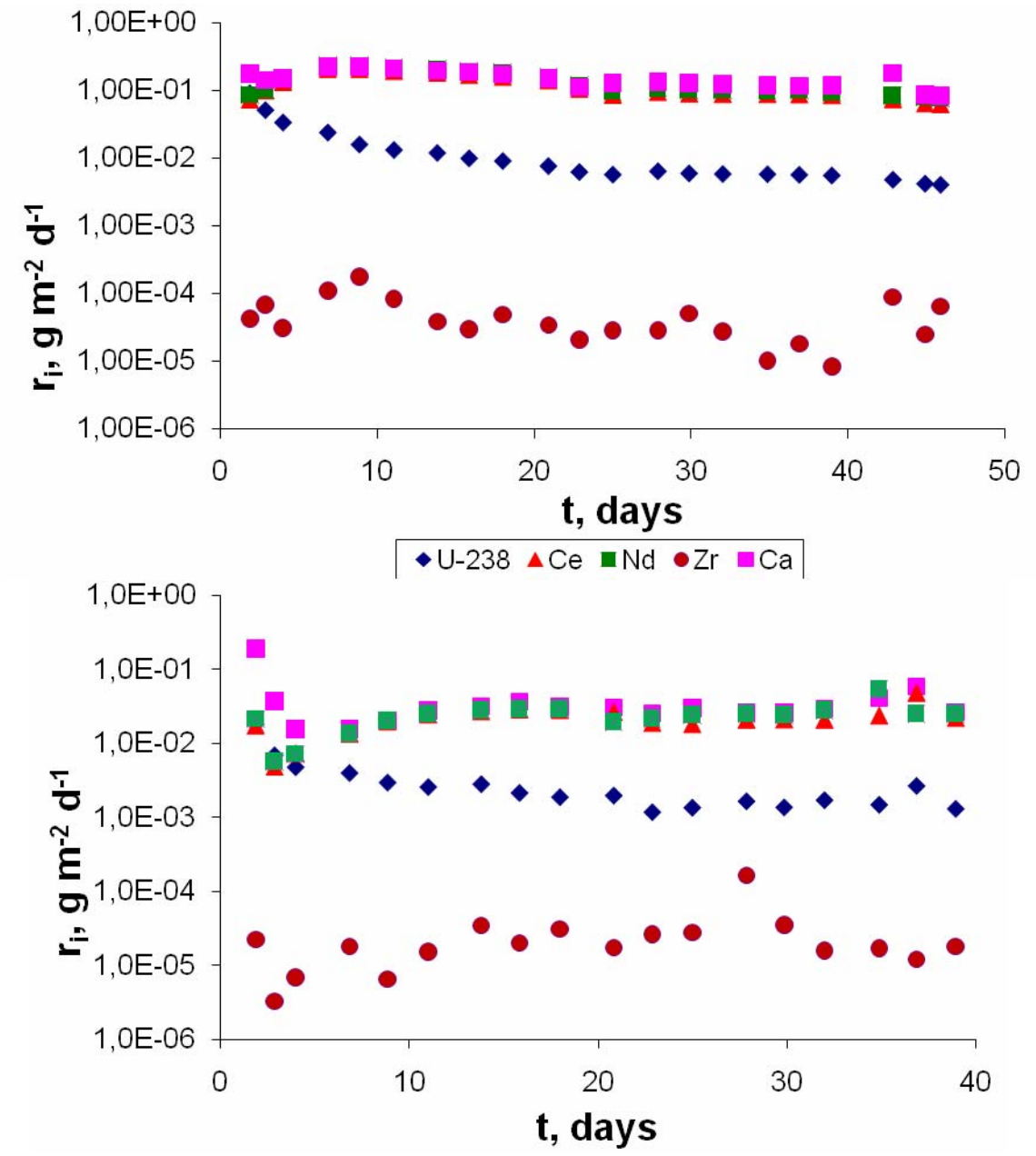

Figure 2. Plots of $\log_{10}$[Leach Rate] versus Test Duration for the Samples 2c and 4c.

Table II. SPFT Test Parameters, Elemental Concentrations and Normalized Elemental Leach Rates from the Ceramic Sample 2c (m = 1135,2 mg, S° = 0,017802 m^2).

t, day	pH (25°C)	Flow Rate			F/S°, m/s	Elemental Concentrations, μg L^{-1}					Normalized Leach Rate, g m^{-2} d^{-1}				
		Target, mL d^{-1}	Actual, mL d^{-1}	Actual, m^3/s		Ca	Ce	Nd	U	Zr	Ca	Ce	Nd	U	Zr
1.83	2.16	72	67.32	7.79E-10	4.38E-08	3294.40	408.89	773.03	210.28	0.34	1.74E-01	7.30E-02	8.61E-02	9.02E-02	2.22E-05
2.83	2.10	72	74.84	8.66E-10	4.87E-08	2399.52	500.89	817.57	106.92	0.05	1.41E-01	9.95E-02	1.01E-01	5.10E-02	3.25E-06
3.94	2.09	72	69.48	8.04E-10	4.52E-08	2736.88	723.32	1238.88	75.64	0.10	1.49E-01	1.33E-01	1.42E-01	3.35E-02	6.84E-06
6.80	2.08	72	71.52	8.28E-10	4.65E-08	3971.49	1102.24	1937.19	52.14	0.27	2.23E-01	2.09E-01	2.29E-01	2.38E-02	1.80E-05
8.82	2.07	72	69.11	8.00E-10	4.49E-08	4067.63	1130.04	2018.96	35.94	0.10	2.21E-01	2.07E-01	2.31E-01	1.58E-02	6.47E-06
11.01	2.10	72	71.75	8.30E-10	4.66E-08	3696.04	1022.87	1816.91	28.75	0.22	2.08E-01	1.95E-01	2.16E-01	1.31E-02	1.52E-05
13.77	2.00	72	71.07	8.23E-10	4.62E-08	3462.22	969.96	1753.09	26.27	0.52	1.93E-01	1.83E-01	2.06E-01	1.19E-02	3.43E-05
15.80	1.99	72	71.60	8.29E-10	4.66E-08	3304.51	894.50	1593.46	21.67	0.29	1.86E-01	1.70E-01	1.89E-01	9.89E-03	1.99E-05
17.95	1.98	72	71.51	8.28E-10	4.65E-08	3055.83	834.44	1514.61	19.83	0.46	1.72E-01	1.58E-01	1.79E-01	9.03E-03	3.10E-05
20.85	2.00	72	69.89	8.09E-10	4.54E-08	2719.69	758.07	1360.86	17.08	0.25	1.49E-01	1.41E-01	1.57E-01	7.60E-03	1.71E-05
22.83	1.99	72	70.38	8.15E-10	4.58E-08	2019.33	565.19	1015.30	13.87	0.39	1.12E-01	1.06E-01	1.18E-01	6.22E-03	2.62E-05
24.96	1.95	72	73.26	8.48E-10	4.76E-08	2230.00	442.67	798.15	12.19	0.42	1.28E-01	8.60E-02	9.68E-02	5.69E-03	2.77E-05
27.83	1.95	72	70.86	8.20E-10	4.61E-08	2410.00	501.92	916.13	14.13	2.39	1.34E-01	9.44E-02	1.07E-01	6.38E-03	1.65E-

															04
29.82	1.95	72	71.01	8.22E-10	4.62E-08	2310.00	477.14	852.73	13.11	0.52	1.29E-01	8.99E-02	1.00E-01	5.93E-03	3.51E-05
31.96	1.93	72	70.13	8.12E-10	4.56E-08	2220.00	477.21	867.56	13.01	0.24	1.22E-01	8.88E-02	1.01E-01	5.81E-03	1.57E-05
34.81	1.97	72	70.15	8.12E-10	4.56E-08	2130.00	472.72	852.98	12.88	0.25	1.17E-01	8.80E-02	9.90E-02	5.76E-03	1.69E-05
36.84	1.95	72	71.54	8.28E-10	4.65E-08	2060.00	459.46	838.32	12.40	0.17	1.16E-01	8.72E-02	9.92E-02	5.65E-03	1.19E-05
38.91	1.99	72	70.33	8.14E-10	4.57E-08	2160.00	454.25	810.80	12.33	0.26	1.19E-01	8.48E-02	9.43E-02	5.52E-03	2.22E-05
42.80	1.94	72	71.29	8.25E-10	4.64E-08	3210.00	390.20	706.21	10.53	0.34	1.80E-01	7.38E-02	8.33E-02	4.78E-03	3.25E-06
44.85	1.95	72	70.72	8.19E-10	4.60E-08	1540.00	341.53	668.39	9.27	0.05	8.56E-02	6.41E-02	7.82E-02	4.18E-03	6.84E-06
45.84	1.93	72	68.85	7.97E-10	4.48E-08	1530.00	339.73	671.21	9.17	0.10	8.28E-02	6.21E-02	7.65E-02	4.02E-03	1.80E-05
Average					**4.60E-08**						**1.50E-01**	**1.19E-01**	**1.33E-01**	**1.55E-02**	**4.85E-05**

Table III. SPFT Test Parameters, Elemental Concentrations and Normalized Elemental Leach Rates from the Ceramic Sample 4c (m = 1184,1 mg, S° = 0,017779 m^2).

t, day	pH (25°C)	Flow Rate			F/S°, m/s	Elemental Concentrations, μg L^{-1}					Normalized Leach Rate, g m^{-2} d^{-1}				
		Target, mL d^{-1}	Actual, mL d^{-1}	Actual, m^3/s		Ca	Ce	Nd	U	Zr	Ca	Ce	Nd	U	Zr
1.82	2.14	72	69.10	8.00E-10	4.50E-08	2855.47	76.93	149.94	33.12	0.34	1.94E-01	1.77E-02	2.15E-02	1.83E-02	2.22E-05
2.83	2.08	72	71.24	8.25E-10	4.64E-08	541.44	20.60	38.39	12.18	0.05	3.79E-02	4.87E-03	5.66E-03	6.92E-03	3.25E-06
3.94	2.09	72	72.73	8.42E-10	4.73E-08	218.02	30.65	48.40	8.24	0.10	1.56E-02	7.40E-03	7.29E-03	4.78E-03	6.84E-06
6.80	2.10	72	71.56	8.28E-10	4.66E-08	224.55	57.73	92.48	7.00	0.27	1.58E-02	1.37E-02	1.37E-02	3.99E-03	1.80E-05
8.82	2.08	72	70.21	8.13E-10	4.57E-08	299.31	85.76	141.19	5.29	0.10	2.07E-02	2.00E-02	2.05E-02	2.96E-03	6.47E-06
10.97	2.01	72	72.26	8.36E-10	4.70E-08	394.25	103.60	170.90	4.47	0.22	2.80E-02	2.49E-02	2.56E-02	2.58E-03	1.52E-05
13.78	2.00	72	69.60	8.06E-10	4.53E-08	464.21	119.35	195.75	5.08	0.52	3.18E-02	2.76E-02	2.82E-02	2.82E-03	3.43E-05
15.80	1.98	72	71.95	8.33E-10	4.68E-08	520.76	121.28	198.05	3.74	0.29	3.69E-02	2.90E-02	2.95E-02	2.15E-03	1.99E-05
17.95	1.99	72	71.54	8.28E-10	4.66E-08	448.16	120.24	196.73	3.29	0.46	3.15E-02	2.86E-02	2.91E-02	1.88E-03	3.10E-05
20.79	1.97	72	72.16	8.35E-10	4.70E-08	431.28	112.62	132.47	3.43	0.25	3.06E-02	2.70E-02	1.98E-02	1.97E-03	1.71E-05
22.84	1.99	72	71.63	8.29E-10	4.66E-08	365.02	80.27	148.08	2.07	0.39	2.57E-02	1.91E-02	2.20E-02	1.18E-03	2.62E-05
24.96	1.97	72	69.63	8.06E-10	4.53E-08	440.00	79.54	168.50	2.44	0.42	3.01E-02	1.84E-02	2.43E-02	1.36E-03	2.77E-05
27.83	1.96	72	72.50	8.39E-10	4.72E-08	370.00	88.05	167.44	2.86	2.39	2.64E-02	2.12E-02	2.51E-02	1.65E-03	1.65E-

															04
29.82	1.96	72	71.28	8.25E-10	4.64E-08	370.00	90.14	166.15	2.41	0.52	2.59E-02	2.13E-02	2.45E-02	1.37E-03	3.51E-05
31.96	1.93	72	70.03	8.10E-10	4.56E-08	430.00	90.61	194.24	3.06	0.24	2.96E-02	2.11E-02	2.82E-02	1.71E-03	1.57E-05
34.85	1.96	72	70.23	8.13E-10	4.57E-08	600.00	103.19	377.85	2.65	0.25	4.15E-02	2.41E-02	5.50E-02	1.48E-03	1.69E-05
36.83	1.94	72	72.14	8.35E-10	4.70E-08	830.00	204.54	169.87	4.64	0.17	5.89E-02	4.90E-02	2.54E-02	2.67E-03	1.19E-05
38.91	1.99	72	72.83	8.43E-10	4.74E-08	370.00	92.36	169.87	2.25	0.26	2.65E-02	2.23E-02	2.56E-02	1.31E-03	1.80E-05
Average		72			**4.64E-08**						**3.93E-02**	**2.21E-02**	**2.39E-02**	**3.39E-03**	**2.73E-05**

XRD patterns of the powdered samples 2c and 4c before and after leaching are shown on Figure 3. The as-prepared sample 2c is composed of major "murataite", perovskite, and crichtonite, and minor Mn/Fe titanate $(Mn,Fe)TiO_3$ (pyrophanite/ilmenite) – see also Table I. After leaching at pH = 2 and T = 90 °C reflections due to murataite, crichtonite, and Mn/Fe titanate phases remained nearly unchanged, whereas peaks due to perovskite phase decreased in intensity.

The as-prepared sample 4c is composed of major murataite, and minor rutile, perovskite and crichtonite – Figure 3 (see also Table I). As follows from SEM/EDS data trace of zirconolite is also present but it cannot be determined by XRD precisely due to low content. In the leached sample 4c perovskite content strongly reduces, whereas reflections due to murataite polytypes and crichtonite are well appeared.

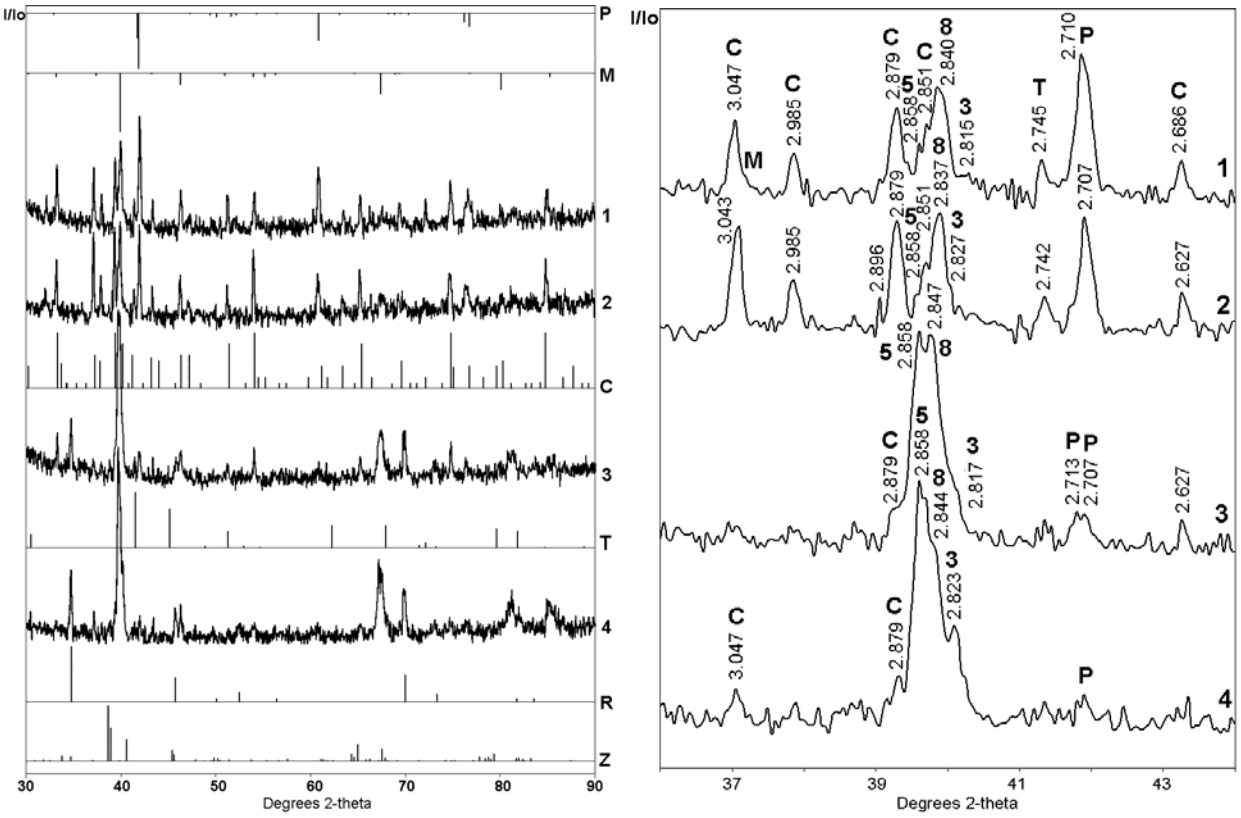

Figure 3. XRD patterns of the ceramics 2c (1,2) and 4c (3,4) before (1,3) and after (2,4) leaching and reference data: P – perovskite, M – murataite (5, 8, and 3 – polytypes with five-, eight-, and three-fold fluorite unit cell, respectively), C – crichtonite, T – pyrophanite/ilmenite, R – rutile, Z – zirconolite (right figure is detail within the range of 36 to 44 degrees 2-theta).

SEM study of the as-prepared samples 2c and 4 c was performed in details earlier and the results were described in our previous paper [4]. As it is seen from Figure 4, the surface of ceramic grains is altered due to corrosion by acid solution (pH = 2). However, no newly formed phases, except supposedly rutile, were revealed because dynamic conditions of the SPFT test exclude accumulation of such phases. Major effect of leachant on the surface of the grains is

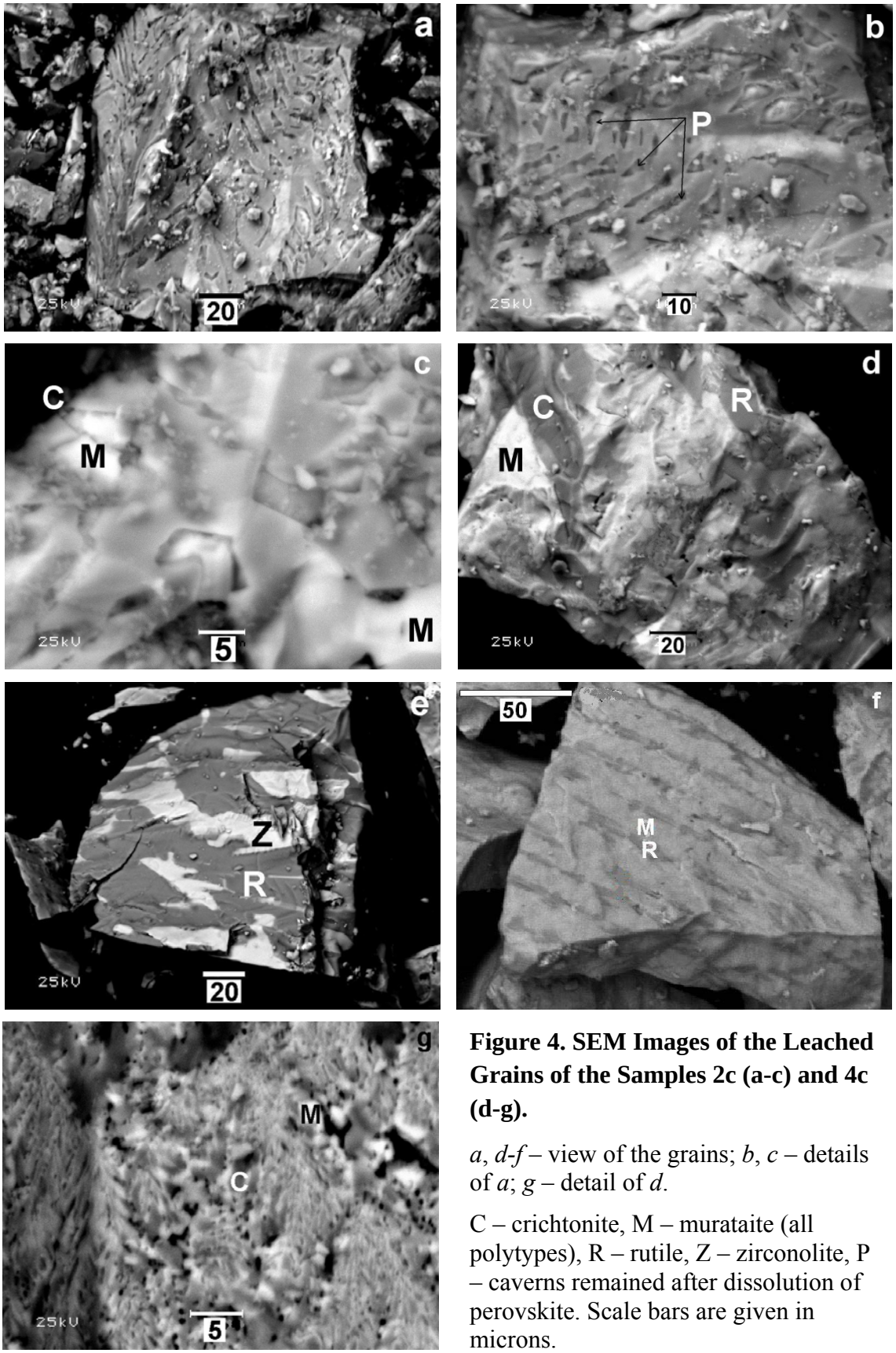

Figure 4. SEM Images of the Leached Grains of the Samples 2c (a-c) and 4c (d-g).

a, *d-f* – view of the grains; *b*, *c* – details of *a*; *g* – detail of *d*.

C – crichtonite, M – murataite (all polytypes), R – rutile, Z – zirconolite, P – caverns remained after dissolution of perovskite. Scale bars are given in microns.

dissolution of the perovskite structure phase resulting in formation of caverns (Figure 4*b*). This process occurs in both the ceramics – 2c and 4c demonstrating that perovskite is the lowest durable phase among titanate waste forms. High values of Ca Ce, and, in some extent, Nd leach rates, especially in the sample 2c, are due to high perovskite content and incorporation of significant fraction of these elements in perovskite, whereas U and Zr enter predominantly murataite polytypes and their leach rates are much lower. Crichtonite and Mn/Fe titanate do not contain U and lanthanides and do not effect of their retention in the ceramics.

In the sample 4c phase assemblage was changed in favor of "murataite" and perovskite content became much lower. As a result, leach rates of Ca, Ce, Nd and U are by 4 to 6 times lower than from the sample 2c. Zr leach rate is also lower than from the sample 2c, but approximately by two times only. This means that Zr enters highly resistant "murataite", at that, major Zr is present in the M5 polytype composing core of the "murataite" grains, and some Zr fraction – in zirconolite, which is one of the most durable phases among actinide and Zr waste forms [7,8].

It is difficult to determine accurately chemical compositions of co-existing phases in the leached samples due to small grain size and non-uniform surface. Approximate compositions are given in Table IV. As expected, contents of high leachable elements, especially those which enter perovskite (Ca, La, Ce, Nd) reduces while contents of lower leachable elements increase or remain at approximately the same level.

DISCUSSION

As it is seen from analysis of experimental data, the highest leach rates were found for the elements (Ca, Ce, in less extent Nd) entering mainly the perovskite phase, which is the lowest durable with respect to acid solution (pH ≈ 2), especially at elevated temperatures (90 °C). The perovskite phase is nearly completely dissolved at leaching under these conditions for several weeks producing caverns on the surface of ceramic grains. The other phases – "murataite", crichtonite, zirconolite (in the sample 4c) are much more durable and only their edges are subjected to leaching yielding Ti-rich phases such as rutile. As far as "murataite" grains are concerned, leachate attacks mainly the M8 polytype composing edges of the "murataite" grains and the M3 polytype (nominal murataite) surrounding them. However, these polytypes are depleted with RE and actinide elements, while the rim composed of the M5 polytype and enriched with these elements is largely protected from leachant attack.

Suppression of perovskite formation by adding of excess TiO_2 and ZrO_2 favors entering RE elements and U the murataite polytypes and some REs, Zr and U enter extra zirconolite. This results in reduction of their leach rates.

SPFT testing at lower leachate flow rate (2 mL d^{-1}) than in our study (~72 mL d^{-1}) were performed for the ceramics designed for excess weapons plutonium immobilization based on different phases – pyrochlore and zirconolite. Normalized forward leach rates of Ce and Gd from pyrochlore-based ceramic was found to be $(5\div8)\cdot10^{-4}$ g m^{-2} d^{-1}, equilibrium state was achieved within ~90 days and equilibrium leach rate were $8.6\cdot10^{-5}$ and $5.9\cdot10^{-5}$ g m^{-2} d^{-1}, respectively. Leach rates of the same elements from ceramic containing extra zirconolite and brannerite increase with time from ~$1.5\cdot10^{-4}$ to $(8\div9)\cdot10^{-4}$ g m^{-2} d^{-1} and equilibrium state in the system was not reached even within 120 days. At higher leachate flow rate (10 mL d^{-1}) leach rates of Ce and

Table IV. Chemical Compositions (wt%) of Co-Existing Phases in the As-Prepared (AP) and Leached (L) Samples 2c and 4c.

Oxides	2c										4c									
	M5		M8		M3		P		C		M		P		C		Z		R	
	AP	L	AP	L	AP	L	AP	L	AP	L	AP	L	AP	L	AP	L	AP	L	AP	L
Al_2O_3	2.9	4.0	4.0	2.6	9.7	5.4	1.2	2.6	6.6	3.8	3.8	4.0	1.6	3.2	6.0	4.5	1.9	2.1	0.8	0.9
CaO	8.0	7.4	9.4	15.1	7.9	3.6	23.3	15.1	3.9	4.5	9.3	8.3	19.7	8.7	4.0	4.7	9.0	8.7	0.7	0.5
TiO_2	47.3	46.1	51.6	54.6	49.5	60.6	48.5	54.6	62.7	65.5	53.3	52.9	50.3	50.0	64.6	64.4	48.0	44.6	88.8	87.7
MnO	12.2	12.6	10.8	4.9	15.4	11.5	1.3	4.9	10.8	10.5	8.9	9.5	2.0	9.1	10.4	8.6	5.9	4.8	0.6	0.5
Fe_2O_3	3.7	3.2	4.1	2.8	6.1	7.2	0.8	2.8	7.2	6.7	4.1	4.4	1.3	4.4	6.7	5.1	2.5	2.1	0.7	0.8
ZrO_2	14.2	15.1	9.0	1.6	4.4	3.6	>>	1.6	3.1	2.5	9.6	9.7	>>	11.7	2.5	3.1	20.9	25.9	8.7	7.6
La_2O_3	*0.5*	2.0	>>	1.9	>>	1.9	2.3	1.9	1.2	2.0	0.6	1.3	3.3	1.7	1.1	2.5	0.2	1.4	>>	*0.5*
Ce_2O_3	2.6	1.8	2.7	3.1	1.8	0.4	5.7	3.1	1.6	0.5	2.6	1.5	6.4	1.5	1.6	1.2	2.1	1.7	>>	*0.1*
Pr_2O_3	*0.7*	*0.2*	*0.7*	2.0	*0.7*	*0.3*	3.6	2.0	*0.5*	>>	0.8	1.6	3.4	0.2	0.7	0.3	0.8	1.2	>>	*0.2*
Nd_2O_3	2.3	2.8	3.0	9.0	1.8	2.2	11.1	9.0	1.7	2.6	3.1	3.7	9.2	4.2	1.5	2.7	4.2	4.3	>>	*0.2*
Sm_2O_3	*0.7*	*0.5*	*0.7*	1.4	*0.5*	*0.7*	1.5	1.4	>>	*0.2*	*0.3*	*0.8*	1.1	1.3	>>	0.9	0.9	0.8	>>	>>
Eu_2O_3	*0.3*	*0.1*	*0.4*	*0.2*	*0.5*	*0.4*	*0.4*	*0.2*	>>	*0.4*	*0.2*	*0.4*	>>	1.0	>>	*0.1*	0.4	*0.3*	>>	*0.2*
Gd_2O_3	*0.3*	*1.2*	>>	*0.2*	>>	*1.7*	*0.4*	*0.2*	>>	*0.6*	>>	*0.9*	>>	1.5	>>	1.3	0.5	0.9	>>	*0.6*
UO_2	4.6	3.5	3.1	0.5	2.3	0.5	>>	0.5	>>	*0.3*	1.4	1.0	>>	1.5	>>	0.5	1.8	1.3	>>	0.2
Total	100.3	100.5	99.5	100.0	100.6	100.0	100.1	100.0	99.3	100.0	98.0	100.0	98.3	100.0	99.1	100.0	99.1	100.0	100.3	100.0

M5, M8, M3 – polytypes of the murataite/pyrochlore series with five-, eight-, and three-fold fluorite unit cell, respectively; P – perovskite, C – crichtonite, Z – zirconolite, R – rutile.
Italics indicates the values lower 2-sigma.
>> - lower than detection limit.

Gd raised by about 10 times [9]. Average values of Y, Gd and Lu leach rates from pyrochlore-based ceramics with target composition $REE_2Ti_2O_7$ (REE = Y, Gd, Lu) at pH = 2, T = 90 °C, and F = 4.8 mL d^{-1} reduced in this row from $1.2\cdot10^{-2}$ to $2.1\cdot10^{-3}$ and $6.2\cdot10^{-4}$ g m^{-2} d^{-1} whereas average Ti leach rate ranged between $2.1\cdot10^{-4}$ and $4.5\cdot10^{-4}$ g m^{-2} d^{-1} and was independent from composition of the ceramics [10].

For the complex $^{239}PuO_2$-bearing (~12 wt.%) pyrochlore-based ceramic containing ~3 vol.% each of zirconolite and rutile the equilibrium state at pH = 2 and T = 90 °C was achieved within ~250 days and equilibrium normalized leach rates of Gd, Ti, Hf, U and Pu were found to be $1.68\cdot10^{-5}$; $2.73\cdot10^{-6}$; $4.04\cdot10^{-7}$; $1.50\cdot10^{-5}$ и $7.62\cdot10^{-6}$ g m^{-2} d^{-1}, respectively [11]. For the ceramic with the same chemical composition but more complex Pu isotopic composition: ~88 % $^{238}PuO_2$, ~11 % $^{239}PuO_2$, ~1 % $^{241}PuO_2$ and received a cumulative dose of $1\cdot10^{18}$ α-decays g^{-1} the normalized leach rates increased by 10 times for Gd and Ti, 570 times for U, and 1450 times for Pu [11]. Normalized leach rates from the ceramics with similar chemical composition but doped with Ce as a Pu surrogate, being leached under conditions similar to those used in our work, were found to be (g m^{-2} d^{-1}): $(1.53\div4.75)\cdot10^{-3}$ for Ce; ~$1.1\cdot10^{-2}$ for Ca; $(1.14\div4.48)\cdot10^{-3}$ for Gd, and ~$1\cdot10^{-3}$ for Ti. Decrease of the flow rate value by ~10 times reduced elemental reach rates by 2.5-5 times [12].

For the ceramics with nominal compositions $Gd_2Ti_{2-x}Zr_xO_7$ equilibrium leach rate of Gd at pH = 2, T = 90°C, and F = 4.8 mL d^{-1} were found to be $1.57\cdot10^{-2}$, $2.20\cdot10^{-2}$, $5.38\cdot10^{-4}$, $1.33\cdot10^{-4}$ and $6.26\cdot10^{-}$ g m^{-2} d^{-1} at x = 0, 0.25, 0.5, 0.75, and 1, respectively [13]. Actually the ceramic at x = 1 was inhomogeneous (polyphase) and it was not determined which phase and in which extent was responsible for leaching of Gd.

Equilibrium elemental leach rates from zirconolite-based ceramic at pH=2, T = 90 °C, F = 20 mL d^{-1} were $(3\div4)\cdot10^{-7}$, $(3\div4)\cdot10^{-6}$, $(4\div5)\cdot10^{-6}$, $(2\div3)\cdot10^{-5}$, ~$2\cdot10^{-5}$ and ~$1\cdot10^{-4}$ g m^{-2} d^{-1} for Ti, Ca, Gd, Ce, ^{239}Pu and U, respectively [5].

As follows from the reference data, there are significant variations in leach rates of the same element depending on leached element, leachant flow rate, method and conditions of sample preparation, phase and chemical composition of the ceramic even at the same pH value and temperature. The lowest elemental leach rates are characteristic of zirconolite- and pyrochlore- based ceramics primarily produced by hot-pressing from sol-gel derived precursor. Therefore, it is rather hard to compare the results obtained in different works. In particular, we did not find reference data on SPFT testing of the zirconolite- and pyrochlore-based ceramics produced via melting/crystallization route, all the more so by CCIM.

In our previous work [14] we studied leaching of Th and U from the samples of murataite-based ceramics with chemical compositions and under conditions similar to those studied in the present work. Equilibrium normalized leach rates of Th and U from the ceramics produced by melting/crystallization of oxide mixtures in a resistive furnace were found to be ~$1.0\cdot10^{-5}$ and $1{,}4\cdot10^{-3}$ g m^{-2} d^{-1}, respectively. Leach rate of Th from the sample produced by CCIM was ~$2\cdot10^{-5}$ g m^{-2} d^{-1}. Thus, average leach rates of Th from murataite-based ceramics produced via melting route at the same pH and T values and from 3.5 to 7 times higher leachant flow rates are similar to those for zirconolite- and pyrochlore-based ceramics produced by cold pressing and sintering at 1350-1500 °C. Equilibrium U leach rates at F = 72 mL d^{-1} from the ceramics produced by melting in resistive furnace (~$1\cdot10^{-3}$ g m^{-2} d^{-1}) and CCIM (~$2\cdot10^{-3}$ g m^{-2} d^{-1} for the sample 4c) are higher by one order of magnitude than those from zirconolite-based [5] and by two orders of magnitude than those from pyrochlore-based ceramics [11] produced by cold pressing and sintering and leached at F ≤ 20 mL d^{-1}. Because, as shown in ref. [9], under the same conditions increase of leachant flow rate by 5 times increases elemental leach rates by one order of magnitude, it should be expected that we will have the same in our case and leach rates of U as well as Ca, Ce and Nd must be lower by about one order of magnitude and become comparable with those from zirconolite- and pyrochlore-based ceramics. Equilibrium leach rate of Zr from the melted samples is the same or lower than that from the sintered samples.

It should be also noted, that elemental leach rates in acid solution (pH = 2) are higher than those under near-neutral conditions (pH = 7-9) typical of underground repository by at least two orders of magnitude. Taking it into account, the most realistic assessment of elemental leach rates from murataite-based ceramics under geological conditions are 10^{-4}-10^{-5} g $m^{-2}d^{-1}$.

Anyway, SPFT data on zirconolite- and pyrochlore-based ceramics are concerned with small samples only produced by sintering of compacted pellets at temperatures as many as 1200 °C followed by re-milling and either sintering at 1500 °C or hot-pressing at 1600 °C under a pressure of 200 MPa. No one sample of such waste forms produced under conditions close to those occurred at actual radiochemical plant. As we have shown earlier [15], phase composition of the pyrochlore-based ceramic produced by cold pressing and sintering at the LLNL bench-scale unit and delivered us for comparative study, was markedly different from the target composition by occurrence of extra perovskite phase. Unfortunately, extra phases (perovskite, crichtonite, rutile, and occasionally zirconolite) are present in the ceramics produced by CCIM as well. Occurrence of the latter three phases does not create appreciable problems from point of view of immobilizing properties of waste forms. Zirconolite is chemically durable and radiation resistant phase and, moreover, its content is negligible. Crichtonite contains traces of RE and actinide elements and is also corrosion-resistant phase. Rutile at high temperatures is able to incorporate minor Zr. Traces of REs and U in EDS analyzes of rutile (Table IV) is due to a capture of surrounding material by electron probe. At the same time, occurrence of perovskite as the lowest durable phase among the titanate actinide matrices increases substantially release of both Ca and light REs (La, Ce, Nd), and, probably, isomorphically incorporated trivalent actinides.

As follows from analysis of the results obtained, in the titanate and aluminotitanate systems with Ce-group lanthanides (La, Ce, Pr, Nd) formation of the perovskite structure phases $(Ca,Ln)(Ti,Al)O_3$ cannot be avoided. It content may be reduced by addition buffer crichtonite-type phase not containing or containing traces of RE and actinide elements as it was done in the present work. An alternative is development of HLW partitioning technology providing for separation of “pure” actinide fraction to be incorporated in quasi-monophasic perovskite-free ceramic.

CONCLUSION

The ceramic with reduced perovskite content was found to be higher corrosion resistant with respect to heated acid solution (SPFT procedure, pH = 2, T = 90 °C, continuous flow of leachate) than that composed of close amounts of murataite, perovskite, and crichtonite. Reduction of perovskite content in the ceramic by about three times decreases normalized leach rates of Ca, Ce, Nd and U by factors of 4 to 6 due to re-distribution of these elements, especially Ce-group REs in favor of the murataite phase. Perovskite being the lowest corrosion resistant phase is released from the surface of the ceramic grains remaining caverns.

ACKNOWLEDGEMENTS

The samples were produced at the Radon lab-scale CCIM unit by Dr. O.A. Knyazev and Ms. M.S. Zen’kovskaya (SIA Radon). Authors also thank Ms. N.P. Penionzkiewiz (SIA Radon) for recording of XRD patterns.

REFERENCES

1. S.V. YUDINTSEV, S.V. STEFANOVSKY, R.C. EWING, "Actinide Host Phases as Radioactive Waste Forms," Structural Chemistry of Inorganic Actinide Compounds, S.V. Krivovichev, P.C. Burns & I.G. Tananaev, eds. (Elsevier B.V., 2007), p. 457-490.
2. T.S. ERCIT, F.C. HAWTHORNE, "Murataite, a UB_{12} Derivative Structure with Condensed Keggin Molecules," Canad. Miner. 33 (1995) 1223-1229.
3. V.S. URUSOV, N.I. ORGANOVA, O.V. KARIMOVA, S.V. YUDINTSEV, S.V. STEFANOVSKY, "Synthetic "Murataites" as Modular Members of the Polysomatic Series Pyrochlore-Murataite," Trans. (Doklady) Russ. Acad. Sci./Earth Sci. Sec., 401 (2005) 319-325.
4. S.V. STEFANOVSKY, A.G. PTASHKIN, O.A. KNYAZEV, M.S. ZEN'KOVSKAYA, O.I. STEFANOVSKY, S.V. YUDINTSEV, B.S. NIKONOV, M.I. LAPINA, "Melted Murataite Ceramics Containing Simulated Actinide/Rare Earth Fraction of High Level Waste," Waste Management 2008 Conf. February 24 -28, 2008, Phoenix, AZ, 2008. ID 8036. CD-ROM.
5. D.M. STRACHAN, R.D. SHEELE, J.P. ICENHOWER, E.C. BUCK, A.E. KOZELISKI, R.L. SELL, R.J. ELOVICH, W.C. BUCKMILLER. "Radiation Damage Effects in Candidate Ceramics for Plutonium Immobilization," Final Report. Pacific Northwest National Laboratory. PNNL-14588 (2004).
6. NUCLEAR WASTE MATERIALS HANDBOOK (TEST METHODS). DOE Technical Information Center. Washington, DC. Report DOE/TIC-11400 (1981).
7. E.R. VANCE, B.D. BEGG, R.A. DAY, C.J. BALL, "Zirconolite-Rich Ceramics for Actinide Wastes," Mat. Res. Soc. Symp. Proc. 353 (1995) 767-774.
8. S.V. STEFANOVSKY, S.V. YUDINTSEV, R. GIERE, G.R. LUMPKIN, "Nuclear Waste Forms," Energy, Waste and the Environment: A Geological Perspective. Geological Society, London, Special Publication, 236 (2004) 37-63.
9. J.P. ICENHOWER, B.P. MCGRAIL, H.T. SCHAEF, E.A. RODRIGUEZ, "Dissolution Kinetics of Titanium Pyrochlore Ceramics at 90 °C by Single-Pass-Flow-Through Experiments," Mat. Res. Soc. Symp. Proc. 608 (2000) 373-378.
10. Y. ZHANG, K.P. HART, M.G. BLACKFORD, B.S. THOMAS, Z. ALY, G.R. LUMPKIN, M.W. STEWART, P.J. MCGLINN, A. BROWNSCOMBE, "Durabilities of Pyrochlore-Rich Titanate Ceramics Designed for Immobilization of Surplus Plutonium," Mat. Res. Soc. Symp. Proc. 663 (2001) 325-332.
11. J.P. ICENHOWER, B.P. MCGRAIL, D.M. STRACHAN, R.D. SHEELE, V.L. LEGORE, E.A. RODRIGUEZ, J.L. STEELE, C.F. BROWN, M.J. O'HARA, "Experimental Determination of the Dissolution Kinetics of Plutonium- and Uranium-Bearing Ceramics at 90 °C," Mat. Res. Soc. Symp. Proc. 713 (2002) 433-440.
12. J.P. ICENHOWER, D.M. STRACHAN, B.P. McGRAIL, R.D. SHEELE, E.A.RODRIGUEZ, J.L. STEELE, V.L. LEGORE, "Dissolution Kinetics of Pyrochlore Ceramics for the Disposition of Plutonium," Amer. Mineral. 91 (2006) 39-53.
13. J.P. ICENHOWER, W.J. WEBER, N.J. HESS S., THEVUTHASEN, B.D. BEGG, B.P. MCGRAIL, E.A. RODRIGUEZ, J.L. STEELE, K.N. GEISZLER, "Experimental Determination of Dissolution Kinetics of Zr-Substituted Gd-Ti Pyrochlore Ceramics: Influence of Chemistry on Corrosion Resistance," Mat. Res. Soc. Symp. Proc. 757 (2003) 227-234.
14. S.V. STEFANOVSKY, G.A. VARLAKOVA, I.V. STARTSEVA, S.V. YUDUNTSEV, B.S. NIKONOV, M.I. LAPINA, "Leach Rates Of Uranium And Thorium From Murataite Ceramics," Radiochim. Acta (2008), in press.
15. S.V. STEFANOVSKY, S.V. YUDINTSEV, B.S. NIKONOV, B.I. OMELIANENKO, A.I. GORSHKOV, A.V. SIVTSOV, M.I. LAPINA, R.C. EWING, "Pyrochlore-Type Phases for Actinides and Rare Earth Elements Immobilization," Mat. Res. Soc. Symp. Proc. 556 (1999) 27-34.